# Supporting Information

## Experimental

### Reagents

Arecoline was purchased from TCI (Shanghai, China), and its stock solution of 0.01M was prepared by dissolving the required amount of arecoline in redistilled water and then kept at 4 ºC in darkness. Melamine ($C_3H_6N_6$) was obtained from Sinopharm Chemical Reagent Corp (China). 10 mg $mL^{-1}$ carbon nanohorns (CNHs) and graphitic carbon nitride solution were prepared with N, N-Dimethylformamide (DMF) and redistilled water, respectively, for the future use .Working solutions were freshly prepared before use by diluting the stock solution. The phosphate buffer solution (PBS) was prepared by mixing stock solution of 0.1 M $NaH_2PO_4$ and 0.1 M $Na_2HPO_4$ and adjusting the pH. Other reagents were of analytical regent grade. The water used for the preparation of the solution was purified using a Water purifier (China) purification system.

### Apparatus

The morphology of the samples was characterized by Scanning electron microscopy (SEM) and Transmission electron microscopy (TEM).Cyclic voltammetry (CV) and Amperometric i-t Curve were performed on a CHI 760 electrochemical workstation (Shanghai Chenhua Instrument Co., China) with a conventional three-electrode cell. An Ag/AgCl electrode (sat. KCl) was used as reference electrode.

A platinum wire and a modified glassy carbon electrode (d=3mm) were used as auxiliary electrode and working electrode, respectively. The pH measurements were carried out on PHS-3C exact digital pH metre (Shanghai Leici Co. Ltd., China), which was calibrated with standard pH buffer solutions. Photoelectrochemical measurements were performed with a homemade photoelectrochemical system.

**Synthesis of CNHs**

CNHs was prepared according to the methods described in the literature.[S1] In a typical process, we used the pure graphite rods ($d$ = 8 mm) as the electrodes, then direct current (DC) arc-discharge was performed in a water-cooled stainless steel collector. The discharge between two electrodes was ignited in buffer gas with the pressure of 400 Torr and kept the current at 120 A. The rods were held at a changeless distance from each other of approximately 1mm according to rotating the cathode when the anode was consumed. Finally, we obtained the graphitic particles which fell down to the bottom of the collector in the arc-discharge process. Successively, 30 mg CNHs was dispersed in 3 mL DMF and stirred for 1 h to ensure CNHs can get a good dispersion, and then its stock solution of 10 mg $mL^{-1}$ was prepared for the subsequent application.

**Synthesis of g-$C_3N_4$ nanosheets**

The synthesis of the g-$C_3N_4$ is similar to that reported in the literature.[S2] In this process, the g-$C_3N_4$ nanosheets were prepared by directly heating $C_3H_6N_6$. Firstly,

8 g white melamine powder was placed into an alumina crucible and heated at 773K for 2 h with a heating rate of 2 K $min^{-1}$. Then the sample heated to 803 K for another 2h in a tube furnace under open air condition. After cooling to room temperature, the light yellow g-$C_3N_4$ sheets were obtained. Afterwards, 20 mg of the prepared g-$C_3N_4$ power was added into 2 mL redistilled water and the suspension was ultrasonicated for 3h to ensure g-$C_3N_4$ can get a good dispersion. Finally, its stock solution of 10 mg $mL^{-1}$ was prepared for the further use.

**Preparation of modified glassy carbon electrode**

Prior to modification, the bare glassy carbon electrode (GCE, 3 mm in diameter） was polished with 0.3 and 0.05μm alumina slurry on chamois leather to produce a mirror-like surface, then washed successively with $HNO_3$-$H_2O$ (1/1, v/v), anhydrous alcohol and doubly distilled water in an ultrasonic bath and dried in air before use. For fabrication of modified electrodes, 3 mg $mL^{-1}$ CNHs solution and 2 mg $mL^{-1}$ g-$C_3N_4$ solution were prepared. With a micropipette, 4 μL of CNHs solution was deposited on the fresh prepared GCE surface, and placed it under an infrared lamp until the solvent was evaporated, after the electrode was cooled to room temperature, 4 μL of g-$C_3N_4$ solution was deposited on the CNHs modified GCE surface, and then dried under infrared lamp and cooled to room temperature.

**Preparation of arecoline sample**

Solution containing arecoline sample was prepared as followed. The fresh areca

nuts were cleaned in a beaker with doubly distilled water. After 1.1617g areca nuts were ground in a clean mortar, the sample and 10 mL ethanol were added into the weighing bottle and then kept at 4 ºC in darkness for 24 h. Then the resulting suspension was centrifuged at 8000 rpm for 10 min and the filtrate was collected for subsequent application. Before experiment, 2 μL sample was added to 2998 μL 0.1 M PBS (pH 9.0) and then analyzed by the same Amperometric i-t Curve procedure as the ARB standard solution. Then, a quantitative ARB stock solution was added into the above measured sample system, and Amperometric i-t Curve was started under the same condition.

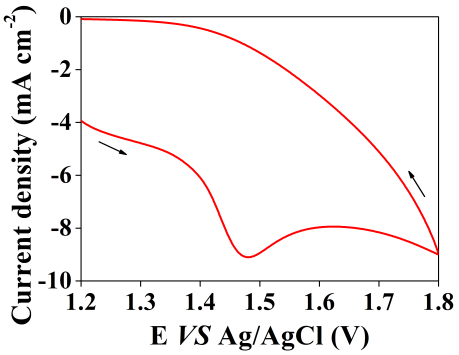


Figure S1 Cyclic voltammograms of AR oxidation at GCE in 0.1 M PBS (pH 9.0) solution with the scan of 100 mV $S^{-1}$.

As shown in Fig. S1, a very large AR oxidation wave with a peak at 1.4 V was observed, which explicit that the AR in PBS solution can be oxide, that is to say, AR served as electron donor in this detection.

**Photochemical and electrochemical stability of g-$C_3N_4$/GCE and CNHs/GCE**

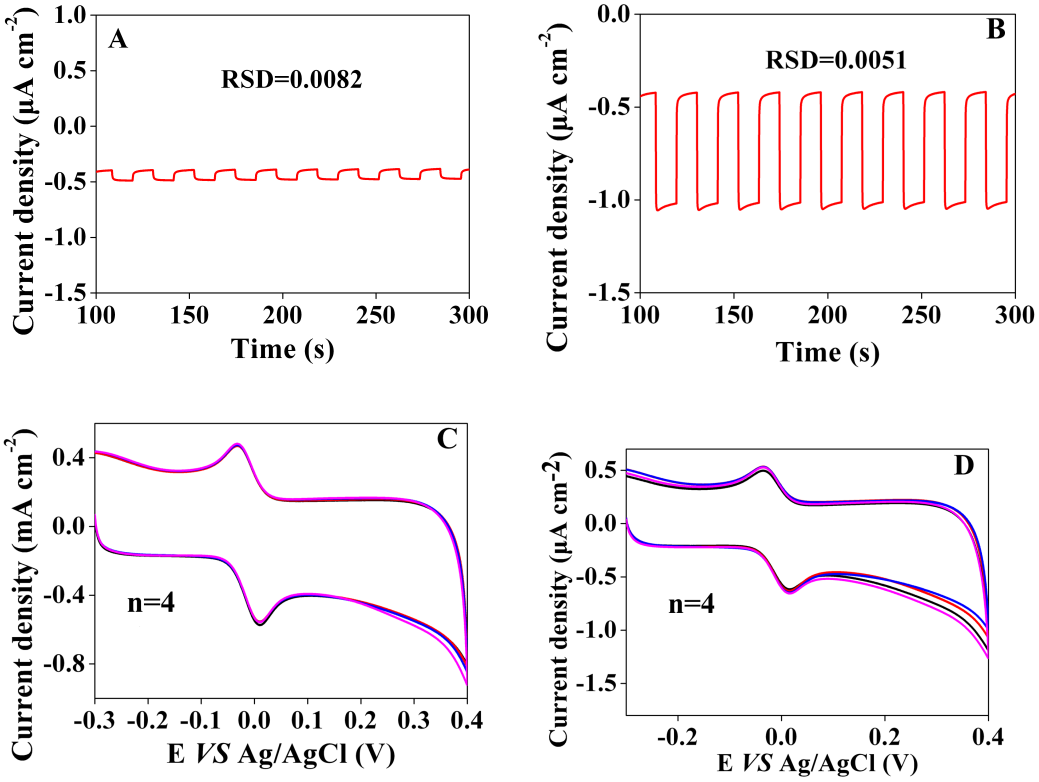


Figure S2 Photocurrent density of (A) CNHs/GCE and (B) g-$C_3N_4$/GCE in 0.1 M phosphate buffer solution (PBS) containing 10 μM AR with light on and off. The applied potential was 0.6 V and the excitation wavelength was 390 nm. (C) CNHs/GCE and (D) g-$C_3N_4$/GCE of 5 mM ferrocene in acetonitrile with 0.1 M tetrabutylammonium perchlorate. Scan rate: 100 mV s-1.

As shown in Fig. S1, the strong and stable photocurrent density of CNHs/GCE (A) and g-$C_3N_4$/GCE (B) were observed with the RSD of 0.82 % and 0.51 %, respectively, suggesting that the modified electrodes have good photochemical stability. Besides, the cyclic voltammograms of the modified electrodes clear indicated that the modified electrodes in 0.1 M PBS (pH 9.0) solution containing 10 μM AR are stable due to there no obvious reduction of peak current in the repeat and

continues scan (as displayed in Fig. S1C and D). This phenomenon proved the electrochemical stability of CNHs and g-$C_3N_4$ nanosheets in the redox electrolytes.

**Parameters optimization**

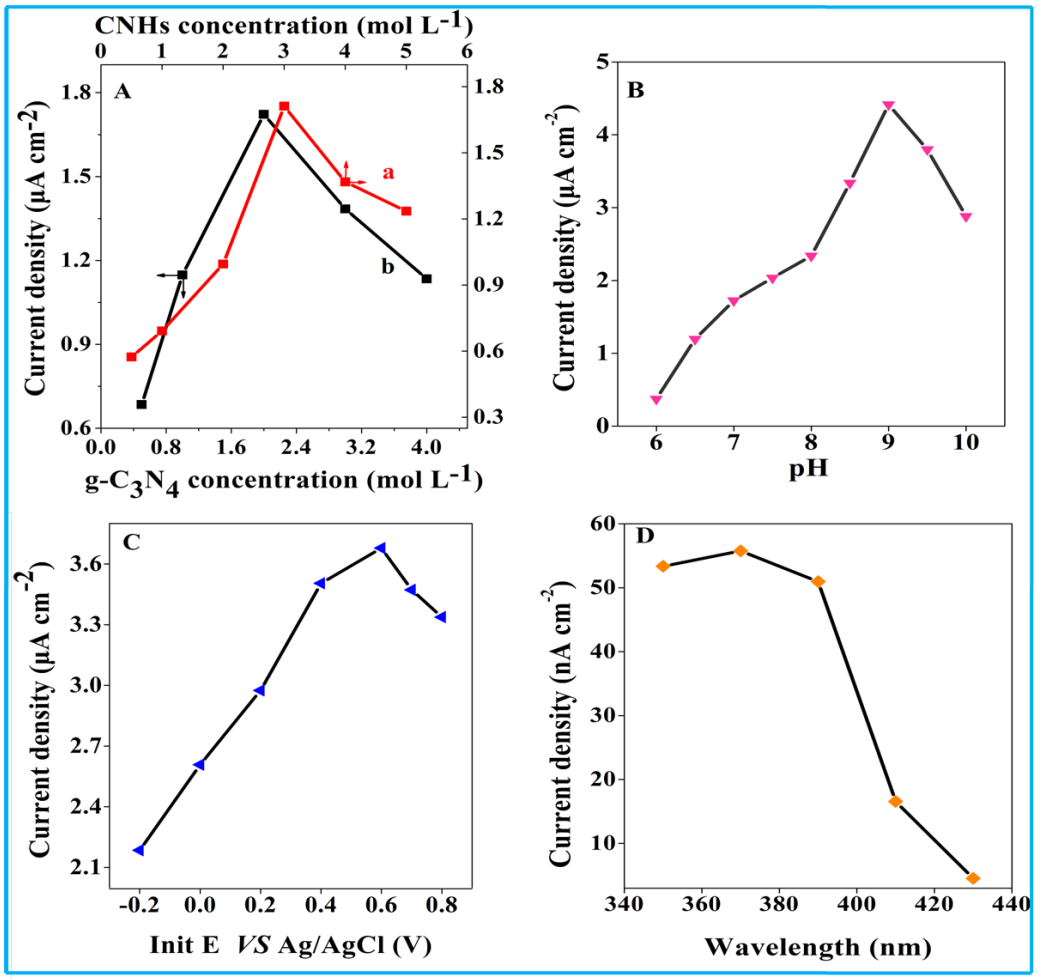


**Figure S3** Effect of (A) the concentration of CNHs (a) and g-C3N4 (b), (B) pH, (C) Init E (*vs* Ag/AgCl), and (D) wavelength to the photocurrent density of CNHs-g-C3N4/GCE electrode in 0.1 M PBS containing 10 μM AR.

**Effect of CNHs concentration**

Fig. S1A (a) depicted the influence of concentration of CNHs on the photocurrent

density in 0.1M PBS (pH 7.0) containing 10 μM AR. Obviously, the photocurrent density increased dramatically with the increasing of the concentration. This is due to the outstanding electrical conductivity of CNHs, with the increasing of the amount, more and more excited electrons were transported from CB of the g-$C_3N_4$ nanosheets to GCE, avoiding electron-hole recombination effectively, resulting in the increasing of photocurrent to light on and off. Whereas, with the concentration increase, photocurrent of the film, reached a peak at 3 mg $mL^{-1}$ and then went down. There were two factors influencing the photocurrent intensity. On the one hand, aggregation of the CNHs made more electron-hole recombination and decreased photocurrent. On the other hand, with the increase of film thickness, the internal resistances increase, which led to the photocurrent decrease. Accordingly, the best concentration of CNHs was selected as 3 mg $mL^{-1}$.

**g-$C_3N_4$ nanosheets concentration effect**

The concentration of g-$C_3N_4$ nanosheets is another important parameter relevant to the photocurrent response. As was shown in Figure S1A (b), the photocurrent density increased with the increasing of the concentration from 0.5 mg $mL^{-1}$ to 2 mg $mL^{-1}$ and then went down significantly. With the amount increasing, photoexcitation was speeding up, which resulted in the increment of the amount of electron-hole pairs on the g-$C_3N_4$ nanosheets. However, at the higher concentration than 2 mg $mL^{-1}$, part of the g-$C_3N_4$ nanosheets would gather together, which lead to excited electron-hole pairs decreased. Moreover, the thicker film inhibited the electron transfer from

g-$C_3N_4$ to CNHs. Consequently, the concentration of 2 mg $mL^{-1}$ was chosen in the following experiments.

**pH effect**

The effect of pH variation on the photocurrent response was investigated in the range 6-10. As it is obvious from Figure S1B that the photocurrent density elevated slowly maximum at pH=9.0 and then decreased with increasing of the pH. It can be explained that the concentration of natural AR reached the maximum at pH 9.0 and more neutral AR can be oxidized. Thus, pH 9.0 was chosen as the optimum pH in the subsequent measurements.

**Init E dependence**

Next, the effect of applied potential on the photoelectrochemical response of the CNHs-$C_3N_4$/GCE toward the detection of the AR was investigated by Amperometric i-t Curve. As demonstrated in Figure S1C, upon addition of 10 μM AR, with an increase of potential from -0.2 V to 0 V (vs. Ag/AgCl), the photocurrent density increased from 2.185 to 2.608 μA $cm^{-2,}$ which was attributed to a negative potential can be inhibit the electron transfer from CNHs-$C_3N_4$ to the electrode, thus lead to electron-hole recombination. With the positive potential increasing, the photocurrent increased resulting from the lower electron-transfer energy barrier. Whereas, the potential in this method was more negative than that of +0.6 V could cause electrochemical oxidization of AR, thus the AR decreased, resulting in the

decrease of the photocurrent. Therefore, 0.6 V was selected as the applied potential for the determination of AR.

**Wavelength effect**

As we know, efficient photocurrent generation needs absorbing light with the energy greater than the band gap. Hence, the wavelength on the photocurrent response was investigated in the range from 350 nm to 430 nm. As was shown in Figure S1D, photocurrent density increased slowly, which was ascribed to the UV absorption of g-$C_3N_4$ at nearly 370 nm. Subsequently, the photocurrent decreased a little from 370 nm to 390 nm and then decreased quickly with the increasing of the irradiation wavelength. Considering that biomolecules may suffer from irradiation with light of excessively short wavelength, 390 nm was chosen for the photoelectrochemical sensing of AR.

**Table S1** Figures of merits of comparable methods for determination of AR

| Method | Analytical ranges (mol $L^{-1}$) | Detection limit (mol $L^{-1}$) | Ref. |
|---|---|---|---|
| Potentiometric method | $5\times10^{-6}$-$10^{-2}$ | $4\times10^{-6}$ | 10 |
| High Performance Liquid Chromatography | $5.5\times10^{-6}$-$8.8\times10^{-4}$ | $3.3\times10^{-6}$ | S3 |
| Capillary electrophoresis-electrochemiluminescence | $10^{-7}$-$10^{-5}$ | $5\times10^{-9}$ | S4 |
| Photoelectrochemical sensor | $10^{-10}$-$10^{-4}$ | $3.3\times10^{-11}$ | This work |

**Table S2** The results of addition recovery test (n=3)

| Content in samples (μmol $L^{-1}$) | Addition (μmol $L^{-1}$) | Measured (μmol $L^{-1}$) | Recovery (%) |
|---|---|---|---|
| 4.57 | 10 | 15.95 | 109.5 |
| 4.57 | 1 | 6.21 | 111.5 |
| 4.57 | 0.01 | 4.68 | 102.2 |

n is the repetitive measurements number

## References

[S1] V. Contini, R. Mancini, R. Marazzi, D. Mirabile Gattia and M. Vittori Antisari, Phil. Mag., 2007, 87, 1123–1137.
[S2] G. Z. Liao, S. Chen, Q. Xie, H.T. Yu and H.M. Zhao, J. Mater. Chem. 22 (2012) 2721-2726.
[S3] Y. N. Yi, X. M. Cheng, L. A. Liu, G. Y. Hu, Z. T. Wang, Y. D. Deng, K. L. Huang, Y. D. Deng, K. L. Huang, G. X. Cai, C. H. Wang, Pharmaceutical Biology, 2012, 50, 832-838.
[S4] Q. Xiang, Y. Gao, B. Y. Han, J. Li, Y. H. Xu, and J. Y. Yin, Luminescence, 2013, 28, 50-55.